Evaluating the seal integrity of natural CO_2 reservoirs of the Colorado Plateau

White S P[1], Allis R G[2], Bergfeld D[3], Moore J N[4], Chidsey T C[2], Morgan C[2], McClure K[2], Adams, M[4], Rauzi S[5],

1 Industrial Research Ltd., PO Box 31-310, Lower Hutt, New Zealand
2 Utah Geological Survey, PO Box 146100, Salt Lake City, Utah 84114
3 USGS, Menlo Park, 345 Middlefield Rd., MS434, California 94025
4 Energy and Geoscience Institute, University of Utah, Salt Lake City, Utah 84108
5 Arizona Geological Survey, Tucson, Arizona 85701

Abstract

The existence of natural CO_2 reservoirs on the Colorado Plateau and adjacent Southern Rocky Mountains confirms that CO_2 can be trapped by favorable structures. Our understanding of these reservoirs is incomplete because data are lacking on the characteristics of the critical sealing units and field measurements of gas leakage rates needed to evaluate the effectiveness of the seals. Mercury injection porosimetry measurements on commonly occurring seal rocks in the Plateau suggest excellent sealing properties, with CO_2 column heights of at least 100 m being supported by samples of the Pennsylvanian Paradox Formation anhydrite, Cretaceous Mancos Shale or Triassic Moenkopi Formation. The main uncertainties about sealing potential arise from whether these units are laterally continuous and not ruptured by permeable fault zones. The presence of many natural CO_2 deposits with multiple, stacked reservoirs highlights the need to carefully evaluate seal integrity and probable CO_2-plume migration paths prior to injection. Preliminary results of soil CO_2 flux measurements over Farnham Dome CO_2 deposits, central Utah show a uniformly low CO_2 flux, and no evidence of seepage from the reservoir. Unusually widespread vein calcite on the ground surface is consistent with a relatively old CO_2 deposit that may have leaked at an earlier time but is now sealed. In contrast, the widespread travertine deposits and a groundwater bicarbonate anomaly over the Springerville-St Johns CO_2 system, eastern Arizona, indicate active leaking of CO_2. Preliminary reactive transport modeling of this

system suggests that travertine deposition, and therefore the CO_2 deposit itself, has probably been present over a timescale of about 10^5 years.

Introduction

The most critical issue confronting acceptance of geologic sequestration of anthropogenic CO_2 is the assurance that most of the CO_2 will stay in the subsurface. Natural CO_2 deposits on the Colorado Plateau provide insights to the characteristics of CO_2 reservoirs and their overlying sealing rocks (Allis et al., 2001). Until recently, the effectiveness of these sealing rocks has received little attention. In this paper we update progress on our study of natural CO_2 deposits on the Colorado Plateau, with emphasis here on seal integrity. In particular, we present results of recent soil gas flux measurements over Farnham Dome CO_2 deposit in central Utah, and contrast these with ongoing work at Springerville-St Johns CO_2 deposit in eastern Arizona-western New Mexico (Fig. 1). At Farnham Dome, recent drilling by Savoy Energy has expanded the known area of the CO_2 deposit to about 15 km^2 suggesting a resource of at least 1.5 TCF (D. Davis, pers. comm.) The source of CO_2 at Farnham Dome has not been determined. There is no obvious natural outflow of CO_2 gas or bicarbonate springs, and no nearby Quaternary volcanism to suggest a recent, juvenile source of CO_2. Deep crustal metamorphism or deep-basin maturation processes are likely sources of CO_2. At the Springerville-St Johns deposit, the proven field covers > 1000 km^2 and contains 14 TCF of CO_2 (S. Melzer, pers. comm.), there are large volumes of travertine at the surface, natural bicarbonate-rich springs and groundwater, and nearby Quaternary volcanics (0.3 – 3 Ma) suggestive of a possible recent deep CO_2 source (Moore et al., in press).

Natural CO_2 reservoirs that are receiving a continual influx of CO_2 may be close to a steady state condition, and therefore may be leaking or spilling CO_2. Leakage without a continual influx of CO_2 gas would deplete the reservoir. Although intermittent recharge and leakage are possible, we suspect the natural CO_2 reservoirs on the Colorado Plateau may be categorized into two states: those that are effectively sealed and preserve CO_2 from an influx at some earlier (geologic) time, and those that are still receiving CO_2 and are leaking or spilling CO_2. The typical rate of CO_2 loss from a reservoir is critical for assessing whether an intermediate, transient state is also likely. Our modeling of the fate of an injected CO_2 plume in a typical Colorado Plateau sedimentary sequence suggests that a steady state condition occurs on a time scale of 10^3 years (White et al., 2003). Given that the Colorado Plateau has

been affected by folding, faulting, burial, dike injection and volcanism occurring on a time scale of 10^7 years, the transient state may be rare.

Preliminary results presented below suggest that Farnham Dome is now a stable, sealed reservoir that was charged with CO_2 at some earlier time, whereas the Springerville-St Johns reservoir is actively leaking CO_2, and may still be receiving CO_2 from depth.

Mechanisms of Reservoir CO_2 loss

CO_2 in the subsurface can exist as gas, as undissociated dissolved CO_2 or as bicarbonate anions in pore water, or it can be precipitated as solid carbonate following reaction with the host rock. Reactive numerical simulation of the fate of an injected CO_2 plume in a typical Colorado Plateau sedimentary sequence has shown that all forms of CO_2 and its reacted products need to be included when considering the transport of CO_2 (White et al., 2003).

Conceptual models of CO_2 loss from a hypothetical reservoir are shown in Fig. 2. Direct leakage of CO_2 gas may occur from the primary reservoir if there are high permeability paths, for example, due to faulting or pinch-out of the low permeability layers on the flanks of a reservoir (Fig. 2a). This type of leakage could also occur at some threshold pressure that causes fractures to open. Alternatively, the capillary pressure constraints of low permeability rocks may limit the vertical extent of a gas column, and leakage occurs once the pressure at the top of the column exceeds a threshold value (Fig. 2b). Very few capillary injection measurements on low permeability formations of the Colorado Plateau have been published (e.g. Jiao and Surdam, 1997 for Cretaceous Laramide Basin units in Wyoming). To supplement the available information, we selected core samples from common low permeability formations in Utah for mercury injection porosimetry measurements. The samples included shales from the Cretaceous Mancos Shale and Triassic Moenkopi Formation, and anhydrite from the Pennsylvanian Paradox Formation. The results are shown in Fig. 3, where they are compared with similar measurements on Paradox Formation carbonate reservoir samples. The results confirm that the seal properties are sufficient to withhold significant volumes of CO_2. The anhydrite effectively has no permeability, the Mancos shale could theoretically hold a CO_2 column from 500 to 900 m in thickness, and the Moenkopi shale could hold a column of up to approximately 100 m. Caution is needed when extrapolating these properties from sample scale to field scale, because the effects of faulting

and fracturing of the trap structure will be important. If the measurements are accepted at face value, then many of the low permeability units on the Colorado Plateau are capable of sealing substantial gas columns (i.e. > 100 m). The uncertainties arise from whether these units are laterally continuous and not ruptured by permeable fault or fracture zones.

Although loss of CO_2 gas may be the most obvious form of leakage from a reservoir, the implications of CO_2 dissolution into pore water make tracking the fate of the CO_2 more difficult. If the CO_2 gas reaches the surface it would be manifest as soil gas anomalies, probably located along faults, or above or close to the leakage or spill points of the reservoir if there is no regional dip to the geological units overlying the reservoir. However, if CO_2 dissolves into pore water, significant lateral transport is possible. Figure 2c shows conceptual scenarios for lateral dispersal of CO_2 from a hypothetical reservoir. Lateral transport may occur in the overlying groundwater regime, within the reservoir itself, or by some combination of flow paths. There are many mechanisms that can affect the ultimate fate of the CO_2, including separation of CO_2 gas from the groundwater (e.g. from decompression effects as fluid rises to the surface, or from "salting out" effects as saline water mixes with CO_2-saturated water), and precipitation or dissolution of carbonate minerals. Some CO_2 could reach the surface, far from the original reservoir, in the form of bicarbonate-rich spring water. Travertine deposits are a likely consequence of CO_2 loss from these fluids as they reach the surface. Some CO_2 could remain in the regional groundwater regime and never reach the surface. A good understanding of the geological structure, the physical properties of the rock units (especially permeability), and the regional groundwater flow regime are needed to fully characterize the possible transport of CO_2 from a reservoir.

Soil Gas Measurements over Farnham Dome, Central Utah

Farnham Dome is a north-south trending anticline approximately 6 km long and 5 km wide. Shale, siltstone and sandstone of the Cretaceous Cedar Mountain Formation are exposed along the crest of the anticline encircled by hogbacks of the overlying Cretaceous Ferron Sandstone Member of the Mancos Shale. Several northeast-southwest trending reverse faults have been mapped along the western portion of the structure (Fig. 4).

Nearly 5 BCF of CO_2 was produced from the Jurassic Navajo Sandstone from 1931 to 1979 when the field was shut in because of a lack of market for the CO_2. CO_2 has also been tested

from the Triassic Sinbad Limestone of the Moenkopi Formation, Permian Kaibab Limestone and Permian White Rim Sandstone. As already noted, recent drilling has extended the known area of the CO_2 resource in the Navajo Sandstone. The Navajo Sandstone is about 80 to 100 m thick, with a 12 m average pay thickness and a 100 m gas column. The Navajo has an average porosity of 12%, an average bottom-hole temperature of 52° C (125°F), and an average gas composition of 99% CO_2 (Morgan and Chidsey, 1991).

The capping unit for the productive eolian Navajo Sandstone is the overlying Jurassic Carmel Formation composed of marine shales and some siltstone and limestone. Other overlying shale units may also help prevent upward migration of CO_2 and promote storage in secondary reservoirs. The role of faults in influencing the extent of CO_2 is unknown. Farnham Dome is located in a broad area of low topographic relief (<100 m), low precipitation (25 cm/y with theoretical transpiration similar in magnitude), and although there is little groundwater data, low lateral flows in the groundwater regime are likely.

A diffuse soil CO_2 survey was carried out across Farnham Dome during April 2004 to determine whether an anomalous CO_2 flux could be detected at the surface, thereby indicating CO_2 leakage and seepage. These measurements were made using a Westsystems flux meter containing a LI-COR 820 infrared gas analyzer (IRGA). The IRGA was calibrated at the start of the field survey using CO_2–free air and 1000 ppm CO_2 standards. IRGA accuracy is reported as <2.5% of the reading, which for this study would indicate a maximum measurement error of 11 ppm. CO_2 measurements are made by placing an accumulation chamber (AC) on the soil surface and pressing it into the soil to obtain a seal. AC gases are pumped through a desiccant to the IRGA and are returned to the AC in a closed loop. CO_2 concentration data were collected for a minimum of 2 minutes at each site. Atmospheric pressure (P) and temperature (T) were recorded at each grid node. The CO_2 flux (F) in units of grams of CO_2 per m^2 per day (g m^{-2} d^{-1}) is calculated using equation 1, where R is the gas constant, V is the system volume, A is the area of the AC footprint, and k is a constant for unit conversion.

$$F = k\left[\frac{P}{RT} \times \frac{V}{A} \times \frac{dc}{dt}\right] \qquad 1$$

Expected measurement errors are reported from laboratory experiments as under-representing actual values by 12% (Evans et al., 2001), or varying by ± 10% (Chiodini et al., 1998).

Fourteen sites were selected over a wide geographic spread and a range of surface geologic units (Fig. 5). Sites included the most deeply exposed section of cover rocks above the reservoir, and potential leakage zones adjacent to known faults. Between 8 and 40 measurements were made at each site along a grid pattern at 25 or 50 m spacing. An arithmetic average soil gas flux was calculated for each site. A summary of the data is given in Table 1, and average fluxes are shown in Fig. 5.

In April, the average soil CO_2 fluxes and the 95% confidence intervals for the grid means were between 0.5 (0.2-0.9) and 3.7 (2.6-4.7) g m^{-2} d^{-1}. Lower fluxes were measured at grids containing soils derived from shales as compared with grids that were sited on sandstone-derived soils. All of the flux values are low and are similar in magnitude (3 g m^{-2} d^{-1}) to soil gas measurements made at Rangely oil field in 2002, where CO_2 injection into an oil reservoir at about 1500 m depth has been occurring since 1986 (Klusman, 2003a, b). In that study Klusman surmises that most of the soil CO_2 is biogenic based on changes in fluxes measured during winter and summer and on isotopic measurements of the near-surface gases. These arid terrain fluxes are lower than soil CO_2 respiration rates of 10 to 20 g m^{-2} d^{-1} from temperate grasslands, croplands and tropical savannas (Raich and Schlesinger, 1992). In similar arid sagebrush terrain, background fluxes of 1 to 5 g m^{-2} d^{-1} have been observed adjacent to the Dixie Valley geothermal field, Nevada (Bergfeld et al., 2001), and at Long Valley, California (Bergfeld, in prep.). For comparison, anomalous fluxes around 55 g m^{-2} d^{-1} have been recorded along the Calaveras fault in California (Lewicki et al., 2003), while average fluxes of ~50 g m^{-2} d^{-1} and 350 g m^{-2} d^{-1} have been measured over the Dixie Valley, and Casa Diablo geothermal fields respectively (Bergfeld et al., 2001; Bergfeld, in prep). Fluxes as high as 50,000 g m^{-2} d^{-1} have been measured at locations around volcanic gas vent areas in Italy (Chiodini et al., 2001).

The very low CO_2 soil fluxes at Farnham Dome are consistent with shallow biogenic CO_2 production alone, and indicate negligible input of CO_2 gas from reservoir depths. Although it is possible that seepage, and therefore leakage, of CO_2 derived from the Farnham Dome reservoir may be occurring at locations that we did capture with our measurements, we suggest that because we surveyed the most likely sites for CO_2 seepage, it is unlikely that

seepage is occurring in this area. The low result for all 14 sites suggests that Farnham Dome may be sealed, and that the CO_2 deposits could have been present for a geologically long time (~10^7 years, perhaps coinciding with the time of maximum burial).

During reconnaissance mapping of the faults and structural trends for site selection for the soil gas measurements at Farnham Dome, widespread calcite veins were noted in shales and joints in sandstone units of the Cedar Mountain Formation (Fig. 6). Areas of vein calcite we noted are shown on Fig. 5, however, because the mapping was not comprehensive, other areas are likely to exist. We believe that these calcite veins reflect past leakage of CO_2 from the Farnham Dome reservoir. Soil gas measurements indicate these zones are now tightly sealed and not leaking.

Evolution of Springerville-St Johns CO_2 Field

The Springerville-St. Johns CO_2 reservoir is largely confined to the Permian Supai Formation, which forms a broad northwest-trending anticline within the field (Figs. 7, 8). Production zones occur primarily in the Fort Apache Limestone, Big A Butte and Amos Wash Members. Some production also occurs from fractured granitic Precambrian basement, and the overlying conglomerates. Wells reportedly produce over 90% CO_2, 5 to 10% N_2, and close to 1% He (Rauzi, 1999).

The area also contains one the greatest concentrations of travertine ($CaCO_3$) spring deposits in the U.S. These deposits cover an area of approximately 250 km^2, primarily south and east of St. Johns (Sirrine, 1956). They are particularly prevalent adjacent to a 10 km length of the Little Colorado River between Lyman Lake and Salado Springs (Fig. 8), where numerous springs and seeps occur today. The fluid source of the travertine deposits appears to be a fault zone, referred to by Crumpler et al., (1994) as the Coyote Wash Fault. None of the springs had temperatures greater than 10°C above ambient in April 2002, and none were exsolving CO_2, although diffusional loss of CO_2 may be occurring (Moore et al, in press). Nevertheless, corrosion of drill pipe by acidic groundwaters and a pronounced HCO_3 anomaly above the CO_2 reservoir provide evidence of a continuing flux of CO_2 from depth (Fig. 9).

Many of the individual travertine deposits are unusually large and symmetric (Fig. 10; Crumpler et al., 1994). Travertine sheets up to 6.4 by 3.2 km in extent and symmetrical circular domes ranging up to 610 m in diameter suggest a long history of CO_2-saturated spring discharge with a nearly constant head from the same vent positions (Sirrine, 1956). The domes typically contain large central chambers that mark the locations of the spring vents.

Dissolution features in the underlying Permian limestones and dolomites suggest much of the $CaCO_3$ deposited as travertine was derived locally. The oldest travertine deposits may have formed during the initial filling of the CO_2 reservoir when carbonate-charged groundwaters exsolved CO_2 upon reaching the surface. The youngest travertine deposits and the present day spring outflows are on the valley floor, about 60 m lower in elevation than the cones of some of the large travertine deposits. There are no dome-like features forming today and the rate of fluid outflow seems to be modest compared to the spring activity implied by the past deposits. These changes suggest a declining pressure regime (Moore et al., in press).

Sirrine (1956) suggests that travertine deposition began in the late Pleistocene after emplacement of the nearby basalts of the Springerville volcanic field. Assuming the travertine deposits now perched 60 m above the valley floor were once at an elevation near the valley floor, an estimate of age is possible if the erosion rate is known. In more deeply incised areas adjacent to the major rivers on the Colorado Plateau, erosion rates of 20 to 40 cm/1000 years have been reported (Biek et al., 2000; Doelling, 1994). However, with the subdued relief of the Springerville-St John area and the relatively small flow of the Little Colorado River here, the erosion rates will be much less. Crumpler et al. (1994) have considered the morphology and state of preservation of the cinder cones in the Springerville volcanic field, which are as young as 0.3 million years and typically about 1 – 2 million years old. The cones are typically well-preserved, and erosion near the upper flanks and central vent areas are shown to be of the order of a few tens of metres. Assuming erosion rates in the Little Colorado River valley to be between a fifth and a tenth that observed in the central Colorado Plateau, the 60 m of erosion since travertine deposition begun could have occurred over a period of the order of 10^5 years. This is similar in magnitude to the age of the youngest volcanism in the area.

The reservoir rocks contain several generations of authigenic minerals, the youngest being kaolinite, which is common, and dawsonite (Fig. 11). Textural relationships indicate that the Al and perhaps Na were derived from the dissolution of detrital feldspars. This dissolution resulted from CO_2 gas charging the reservoir (Moore et al., in press). Interactions between the reservoir rocks and groundwaters from the CO_2 field were simulated. Chemical equilibria calculations indicate that dawsonite will not precipitate until the CO_2 fugacity reached 20 bar, but that kaolinite becomes saturated at lower pressure. The deposition of dawsonite occurred locally where CO_2 was trapped below low permeability seals and where pressures were high enough. Kaolinite may have formed contemporaneously in poorly sealed regions of the reservoir where CO_2 pressures were lower. As the CO_2 pressures declined, dawsonite was overprinted by kaolinite.

Modeling Mineralogical Changes in the Springerville-St Johns CO_2 System

In order to understand the changes suggested by geologic evidence, we have begun modeling the hydrology of the system, including the reactive chemistry of the rock-fluid interactions on a broad scale. This modeling is still in progress and the results presented here are the first stage and are preliminary. A TOUGH2/ChemTOUGH2 (White et al., 2004) integrated finite difference model of the cross-section shown in Figure 8 has been developed representing earlier topography. In this first modeling phase we investigate the main phase of travertine deposition prior to erosion by the Little Colorado River, which acts as a pressure control on the cross-section. This model has the present geographic position of the Little Colorado River raised by about 60 meters to better represent the topography when the travertine mounds were formed. The cross-section is divided into elements with the element geometry determined by the need to reproduce interfaces between the geological layers (Figure 12) and is refined around the fault location.

Boundary Conditions

Boundary conditions for the numerical model are

- Atmospheric pressure at the surface
- 0.3 cm annual infiltration
- Constant hydrostatic pressure on both the vertical boundaries
- No fluid flow through the base of the model

- Heat flow at the base of the model is set to match the typical terrestrial heat flow for the region.

Parameters

Capillary pressure functions

Capillary pressure functions for the seal rocks within the Colorado Plateau are discussed elsewhere in this paper. Curves shown in Figure 3 are used in the numerical modeling.

Permeability

CO_2 in the field is contained in the Permian Supai Formation, the structure of which can be subdivided into four members, Corduroy, Fort Apache, Big A Butte and Amos Wash. There are multiple impermeable anhydrite and mudstone layers within these formations leading to vertical segregation of the CO_2 into several zones. It is not possible to represent all the anhydrite layers in the numerical model, however the two largest regions of anhydrite are included as low permeability layers in the Fort Apache and Big A Butte Members. There is a major fault in the vicinity of the CO_2 field that is represented in the model as a vertical region of high permeability cutting through the horizontal rock units. Parameters adopted for permeability and porosity are given in Table 2. These parameters are based largely on earlier modeling work at Farnham dome (White et al. 2003, 2004)

Mineralogy

We have included sufficient geochemical complexity to represent the interaction of a simplified reservoir mineralogy (Table 3) with CO_2-rich water. Initial chemical conditions were calculated by first assigning the mineralogy specified in Table 3 to model elements, setting the reservoir fluid to a 0.03 M NaCl water, and then allowing the water to react with the reservoir for 1000 years. This modified the original mineralogy slightly and provided initial conditions for the fluid reservoir throughout the reservoir. Not all minerals were in equilibrium after this simulation period; however, it provided an initial chemistry for a full reactive transport model.

Simulation Scenarios

Two simulations were performed. In the first, water-rock interactions were ignored and a constant flux source of CO_2 was added at the base of the model beneath the location of the CO_2 reservoir. This model was then run for about 10^5 years, sufficient time for CO_2 deposits

to accumulate. Deposit locations are shown in Figure 13, two lower deposits in the Supai Formation capped by layers of anhydrite, and a third shallower deposit capped by the Moenkopi and Chinle Formations. The reservoir temperature shown in Figure 14 indicates the existence of a weak, convective upflow where isotherms are pulled upwards. Flows to the surface are small over most of the model; however, one significant flow occurs from the fault zone associated with the travertine mounds and a second flow occurs 30 km to the NW of this. Flow from the fault is about 80 kg/s, which can be compared with a present day flow at Salado Springs of about 10 kg/s (April 2002 estimate). A much larger historic outflow was likely during deposition of most of the travertine.

A second simulation was performed with ChemTOUGH2 to investigate likely chemical changes as a result of the CO_2 deposits developed in the first set of simulations. The initial chemical concentrations calculated from reaction of reservoir minerals with a NaCl water were modified by adding CO_2 either as a gas or dissolved in the reservoir fluid, consistent with the calculated reservoir locations and CO_2 partial pressures. This system was then simulated for a period of 800 years.

Results of the chemical transport simulation are presented in Figures 15-19, and show that calcite is in equilibrium with the reservoir fluid throughout most of the model. This is partly a result of initially having calcite in all formations. The model predicts there may also be some dissolution of detrital plagioclase (modeled as anorthite and albite) and precipitation of calcite in regions of high CO_2 concentration. Dolomite is saturated in areas of high CO_2 concentration and slightly undersaturated in other areas of the model while gypsum is undersaturated throughout the model.

Dawsonite is undersaturated throughout most of the modeled area apart from the deep region with a high CO_2 concentration. The regions of dawsonite precipitation are shown in Figure 19. As with dolomite, dawsonite is largely found in the deep area of the model with a high concentration of CO_2 and also above the region of convective upflow.

These predictions of mineral saturation are in general agreement with the experimental observations, although the calculated gypsum concentrations are significantly lower than those observed. Water flowing to the surface has a total calcium concentration of 0.0165 M and is saturated in CO_2. If all this calcium precipitates as travertine with an average pore

volume of 50% (accounting for the central chambers, Sirrine 1956), and as deposits covering 30% of the outflow area, then this will produce a deposit approximately 10 m thick in a period of 10^5 years.

Although we have not yet estimated the volume of travertine in the system, our field observations suggest that thicknesses are between less than 10 and 20 m. This implies deposition over ~ 10^5 years, and is consistent with the inferred local erosion rates. Erosion has left the travertine domes and sheets perched up to 60 m above the present valley floor. The deposition period is also consistent with the youngest ages of the nearby basaltic cones assuming the volcanism is related to the influx of CO_2.

Conclusions

Investigations of the Farnham Dome and Springerville-St Johns CO_2 fields indicate very different leakage histories. Both reservoirs contain economic amounts of CO_2, are relatively shallow (~ 500 m) and developed in similar sedimentary rocks. Farnham Dome is currently sealed and exhibits no apparent leakage and seepage of CO_2. However, widespread vein calcite in exposed joints and fault zones suggests that the system leaked in the past before it became sealed. There is no Pliocene or younger volcanic activity in the region, suggesting that the CO_2 may be derived from metamorphic processes or maturation of organic matter. If these processes coincided with the time of maximum in the basin, then this CO_2 field could be ~ 10^7 years old.

Springerville-St Johns field is an example of a young, leaking CO_2 system, most likely along a Quaternary fault zone that bounds western side of the system. Spectacular travertine deposits covering an area of 250 km^2 record evidence of CO_2 migration and leakage along this fault zone. These domes occur up to 60 m above the present day valley floor where the youngest carbonate deposits are associated with active bicarbonate springs. Present day groundwater near the field is enriched in bicarbonate and is locally acidic as indicated by corrosion of drill pipes. These features suggest a persistent flux of CO_2 from depth. Petrographic studies of core indicate fluid-rock reactions have resulted in dissolution of carbonates and feldspars, and the deposition of kaolinite and dawsonite, a mineral considered to be significant in CO_2 sequestration.

Reactive chemical transport models of the Springerville-St Johns system are largely consistent with the inferred early hydrology. Dawsonite is predicted to precipitate in areas of high CO_2 partial pressure, whereas kaolinite is near equilibrium throughout the system. However, only a small percentage of the CO_2 is naturally trapped as carbonate minerals. Most CO_2 is stored as a free gas and as dissolved carbonate species in the groundwater. High historic spring discharge rates close to ten times present-day rates are predicted. These rates are sufficient to deposit the observed large volumes of travertine over a time scale of $\sim 10^5$ years. This is a similar to the inferred time scale of local erosion, and to the age of youngest volcanic activity. Most of the travertine may have been derived from dissolution of underlying Permian carbonate units.

Acknowledgements

We thank Dan Davis for informal comments about the implications of the new CO_2 well at Farnham Dome, and Stephen Melzer for informal comments about the Springerville-St Johns CO_2 field. Dave Langton (EGI) and Tom Dempster (UGS) assisted with the soil gas measurements at Farnham Dome. Support for this project was provided by a grant from the Department of Energy (#DE-FC26-00NT4096, Program Manager David Hyman), and cost share came from EGI, UGS, USGS and the New Zealand Foundation for Research, Science and Technology. The mercury injection porosimetry measurements were carried out under contract to TerraTek. David Tabet and Jennifer Lewicki are thanked for critically reviewing earlier versions of the manuscript.

References

Allis, R.G., Chidsey, T., Gwynn, W., Morgan, C., White, S.P., Adams, M., and Moore, J. 2001. Natural CO_2 reservoirs on the Colorado Plateau and Southern Rocky Mountains: candidates for CO_2 sequestration. Proc. 1st National Conference on Carbon Sequestration, May 14-17, 2001, Washington DC, DOE-NETL CD DOE/NETL-2001/1144.

Bergfeld, D., Goff, F. and Janik, C.J., 2001. Elevated carbon dioxide flux at the Dixie Valley geothermal field, Nevada; relations between surface phenomena and the geothermal reservoir. Chem. Geol. 177 (1-2), 43-66.

Biek, R.B., Willis, G.C., Hylland, M.D. and Doelling, H.H. 2000. Geology of Zion National Park, Utah. *In*: Geology of Utah's Parks and Monuments, Editors, Sprinkel, D.A., Chidsey, T.C., and Anderson, P.B., Utah Geological Association Publication 28, 107 – 138.

Chiodini, G., Cioni, R., Guidi, M., Raco, B. and Marini, L., 1998. Soil CO_2 flux measurements in volcanic and geothermal areas. Appl. Geochem. 13 (5), 543-552.

Chiodini, G., Frondini, F., Cardellini, C. Granieri, D., Marini, L., and Ventura, G. 2001. CO_2 degassing and energy release at Solfatara volcano, Campi Flegrei, Italy. J. Geophys. Res. 106, B8, 16,213-16,221.

Crumpler, L.S., Aubele, J.C. and Condit, C.D. 1994. Volcanoes and neotectonic characteristics of the Springerville volcanic field, Arizona. Arizona Geological Society Guidelbook, 45th field conference, Mogollon Slope, west-central New Mexico and east-central Arizona, 147-164.

Doelling, H. 1994. Tufa deposits in west Grand County. Utah Geological Survey "Survey Notes", 26, 2-3, 3 p.

Evans, W.C., Sorey, M.L., Kennedy, B.M., Stonestrom, D.A., Rogie, J.D. & Shuster, D.L. 2001. High CO_2 emissions through porous media: transport mechanisms and implications for flux measurement and fractionation. Chem. Geol. 177 (1-2), 15-29.

Jiao, Z.S. and Surdam, R.C. 1997. Characteristics of anomalously pressured Cretaceous shales in the Laramide Basins of Wyoming. In, R.C. Surdam, ed., Seals, Traps, and the Petroleum System. AAPG Memoir 67, 243-253.

Klusman, R.W. 2003a. A geochemical perspective and assessment of leakage potential for a mature carbon dioxide-enhanced oil recovery project and as a prototype for carbon dioxide sequestration; Rangely field, Colorado. Amer. Assoc. Pet. Geol., 87, 1485-1508.

Klusman, R.W. 2003b. Rate measurements and detection of gas microseepage to the atmosphere from an enhanced oil recovery/sequestration project, Rangely, Colorado, USA. App. Geochem., 18, 1825-1838.

Lewicki, J.L., Evans, W.C., Hilley, G.E., Sorey, M.L.,Rogie, J.D., and Brantley, S.L., 2003. Shallow soil CO_2 flow along the San Andreas and Calaceras Faults, California. J. Geophys. Res. 108, B4 doi:10,1029/2002JB002141,2003

Moore, J., Adams, M., Allis, R., Lutz, S., Rauzi, S., 2004. Mineralogical and geochemical consequences of the long term presence of CO_2 in natural reservoirs: An example from the Springerville-St. Johns field, Arizona and New Mexico, U.S.A. Chemical Geology, in press

Morgan, C.D., and Chidsey, T.C., Jr., 1991. Gordon Creek, Farnham Dome, and Woodside fields, Carbon and Emery Counties, Utah, *in* Chidsey, T.C., Jr., editor, Geology of east-central Utah: Utah Geological Association Publication 19, 301-309.

Raich , J.W., and and Schlesinger, W.H., 1992. The global carbon dioxide flux in soil respiration and its relationship to vegetation and climate. Tellus, Ser. B, 44, 81-99.

Rauzi, S.L. 1999. Carbon dioxide in the St Johns-Springerville area, Apache County, Arizona. Arizona Geological Survey Open-File Report 99-2.

Sirrine, G.K. 1956. Geology of the Springerville-St Johns area, Apache County, Arizona: University of Texas, Austin, unpublished PhD dissertation, 248 p.

Weiss, M.P., Witkind, I.J. and Cashion, W.B. 1990. Geologic map of the Price 30' x 60' quadrangle, Carbon, Duschene, Uintah, Utah and Wasatch Counties. Misc. Investigations Series, USGS.

White, S. P., Allis, R.G., Chidsey T., Moore, Morgan, C., Gwynn, W.J. and Adams, M. 2003. Injection of CO2 into an unconfined aquifer beneath the Colorado Plateau, central Utah. Proc. 2nd Annual Conference on Carbon Sequestration, May 5-8, 2003, Washington DC, NETL-DOE.

White, S. P., Allis, R.G., Chidsey T., Moore, Morgan, C., Gwynn, W.J. and Adams, M. 2004. Simulation of reactive transport of injected CO_2 on the Colorado Plateau, Utah, USA. Chemical Geology, in press.

Witkind, I.J. 1979. Reconnaissance geologic map of the Wellington quadrangle, Carbon County, Utah. Misc. Investigations Series, USGS.

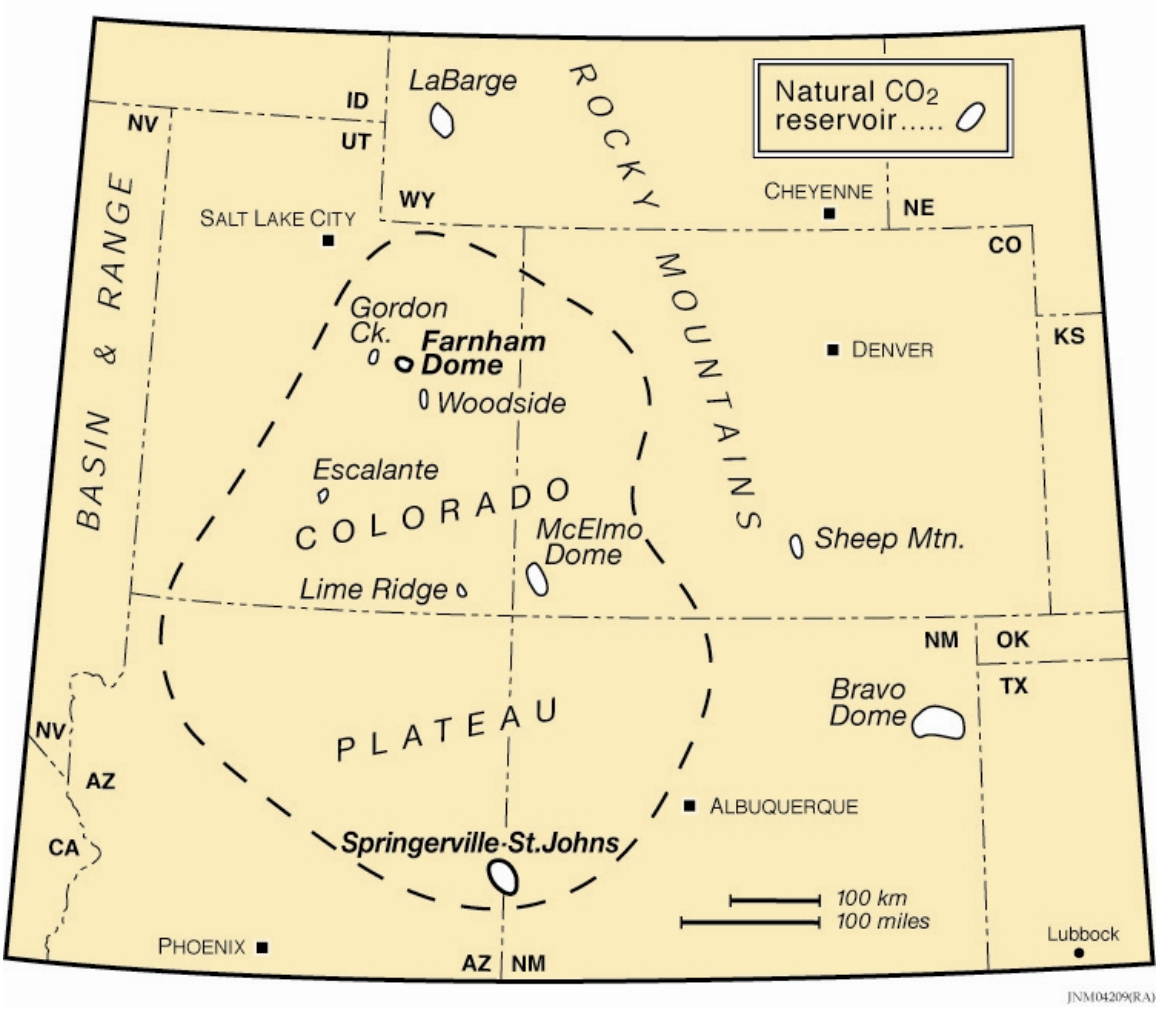

Figure 1. Location of natural CO2 reservoirs within the Colorado Plateau and Southern Rocky Mountains region of the U.S. The two fields of Farnham Dome (Utah) and Springerville-St Johns (Arizona-New Mexico, which are the subject of this paper, are highlighted.

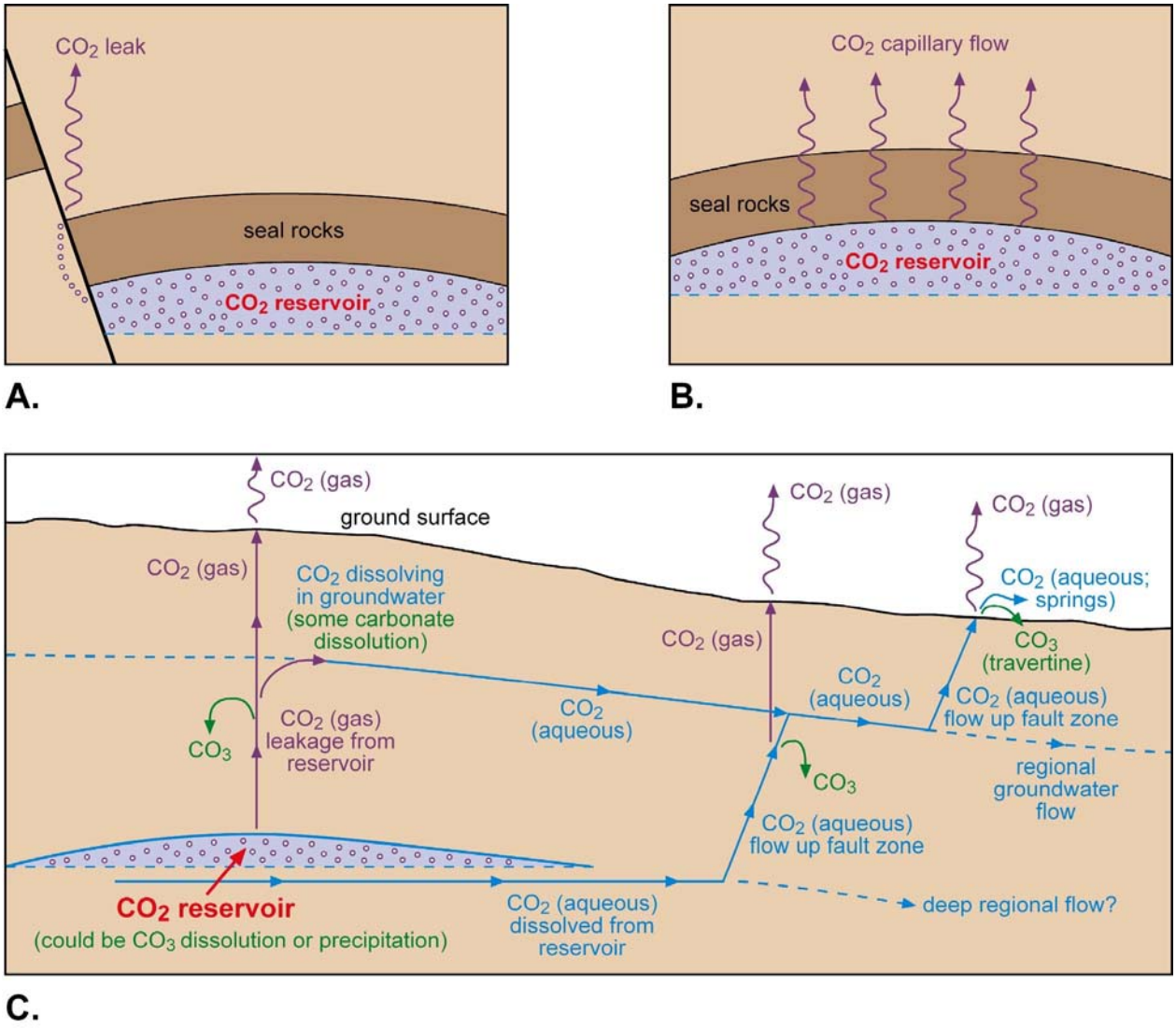

Figure 2. Conceptual illustrations of mechanisms of transport from CO_2 reservoirs. (A) and (B) contrast leakage of gas through seals when capillary pressures are exceeded versus leakage or spilling on fractures and faults. The leakage on faults or fractures could occur when a critical pressure is exceeded. (C): hypothetical lateral flow paths when CO_2 gas is dissolved in the pore water. CO_2 (aqueous) is dissolved CO_2, CO_3 represents carbonate deposition.

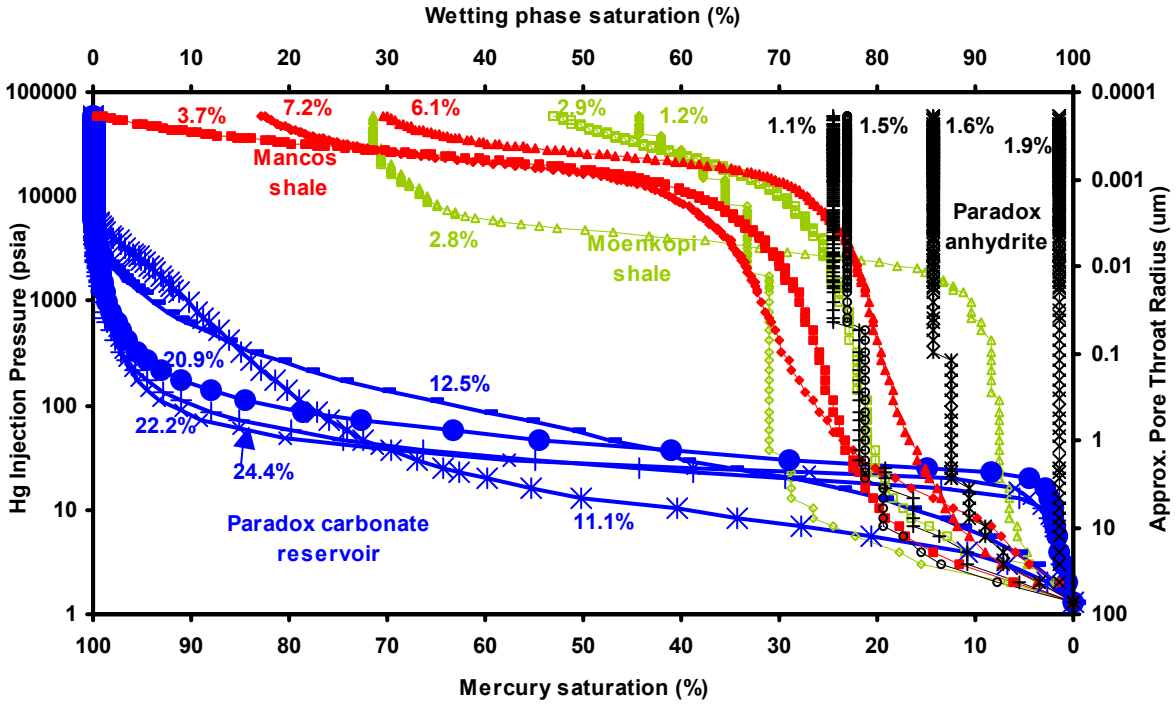

Figure 3. Capillary pressure curves for some of the potential seal units (Moenkopi Formation, Mancos Shale, Paradox anhydrite) and a reservoir unit (Paradox carbonate) of the Colorado Plateau. Percentages next to the curves are the initial porosity of the core sample.

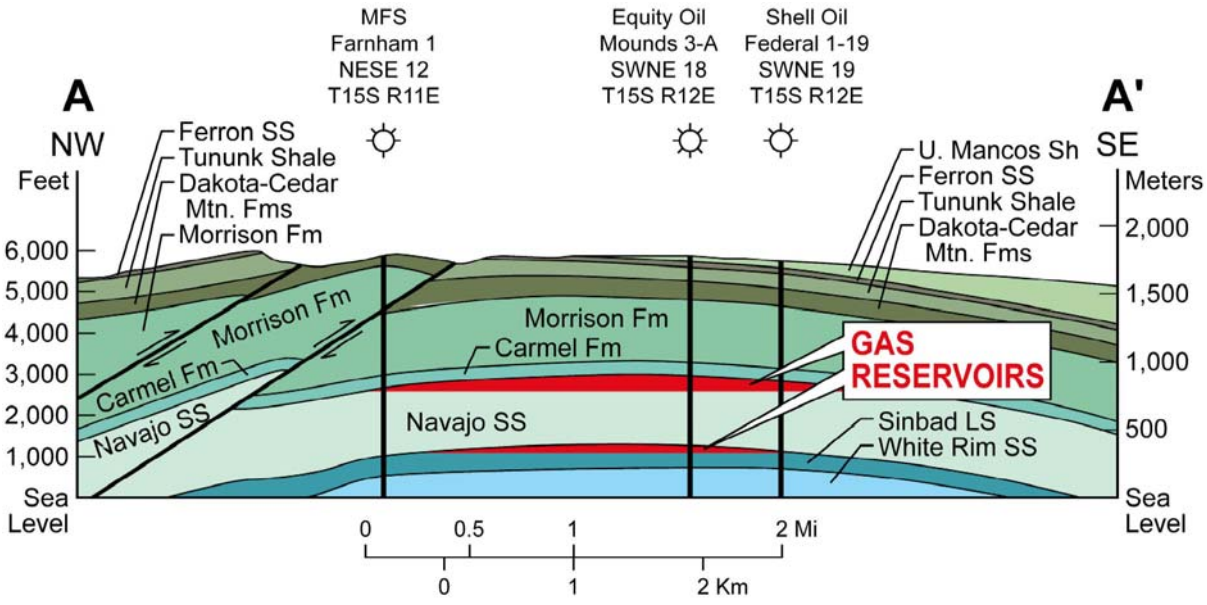

Figure 4. Simplified geologic cross-section of Farnham Dome, Utah. Other faults may be present.

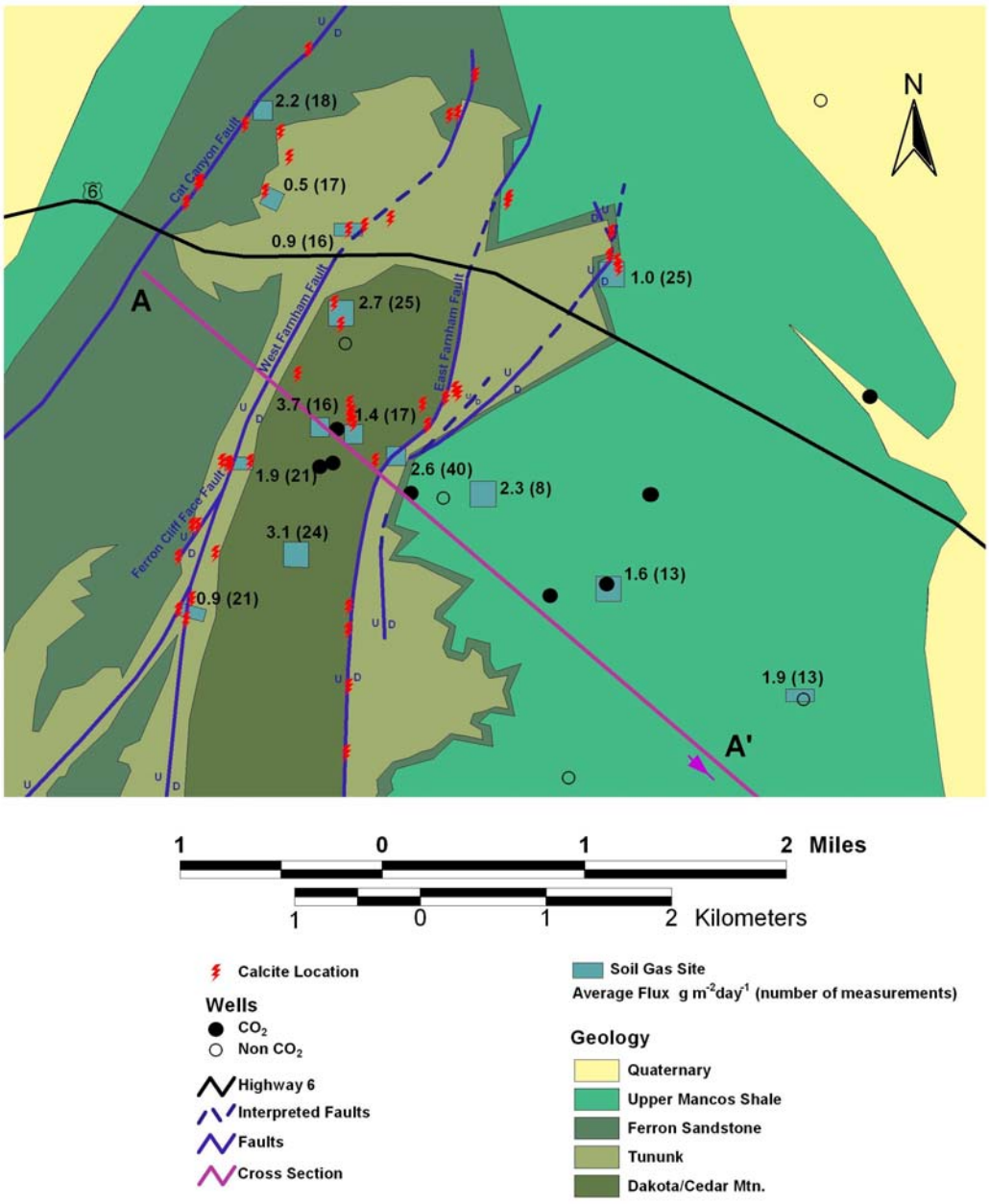

Figure 5. Soil gas flux results from the Farnham Dome CO_2 field area. Flux values are in g m^{-2} d^{-1} and the number of measurements at each site is shown brackets. Faults, CO_2 wells, and prominent calcite occurrences on the ground surface are also highlighted. The geology map is derived from Witkind (1979) and Weiss et al. (1990).

Figure 6 Photos from Farnham Dome showing example of a calcite-lined ridge in Tununk shale (A). A close-up of the calcite fragments in (B) shows alignment of the vein lineations in the larger fragments, suggesting the veins are locally at least 30 cm wide.

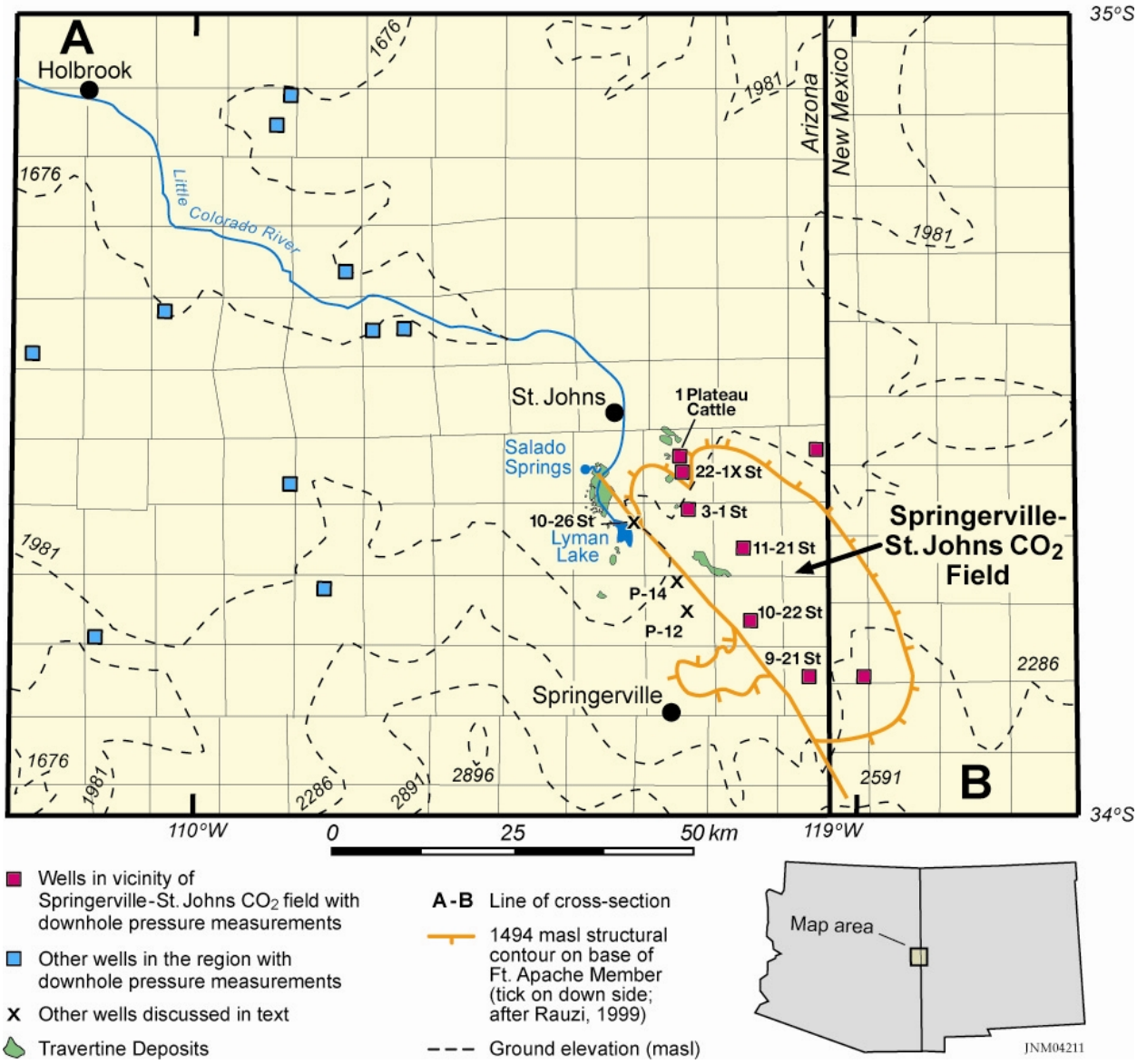

Figure 7. Location of the Springerville-St. Johns CO_2 deposit, with some CO_2 wells and the structural high highlighted. The CO_2 is trapped within a structural high, as indicated by a structural contour on the Fort Apache Member of the Supai Formation. A fault zone (Coyote Wash Fault, Crumpler et al., 1994) appears to form the southwestern limit of the structure.

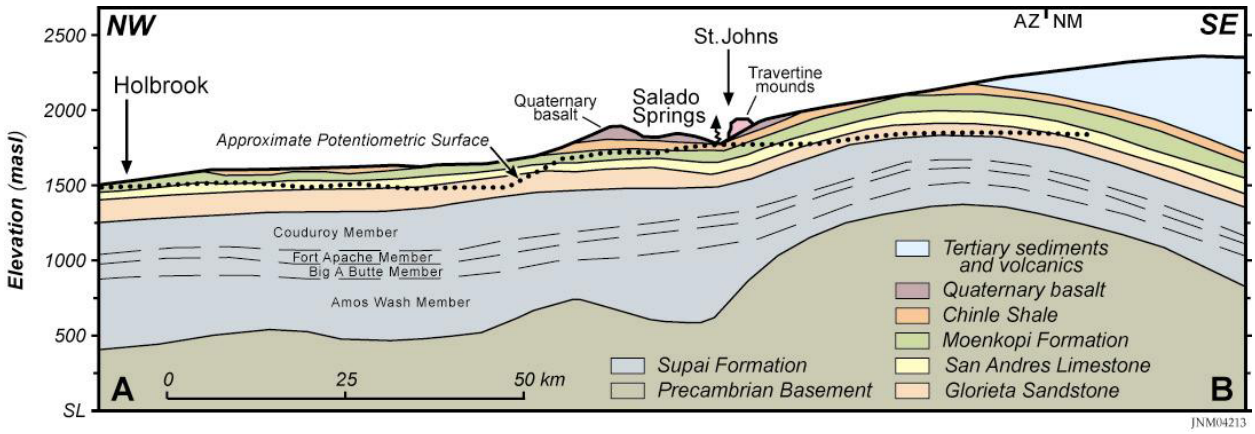

Fig 8. Northwest-southeast cross-section of the Springerville-St Johns area. See Fig. 8 for the location of the cross-section. The CO_2 reservoir is confined to the Supai Formation within the structural high on the southeast end of the cross-section.

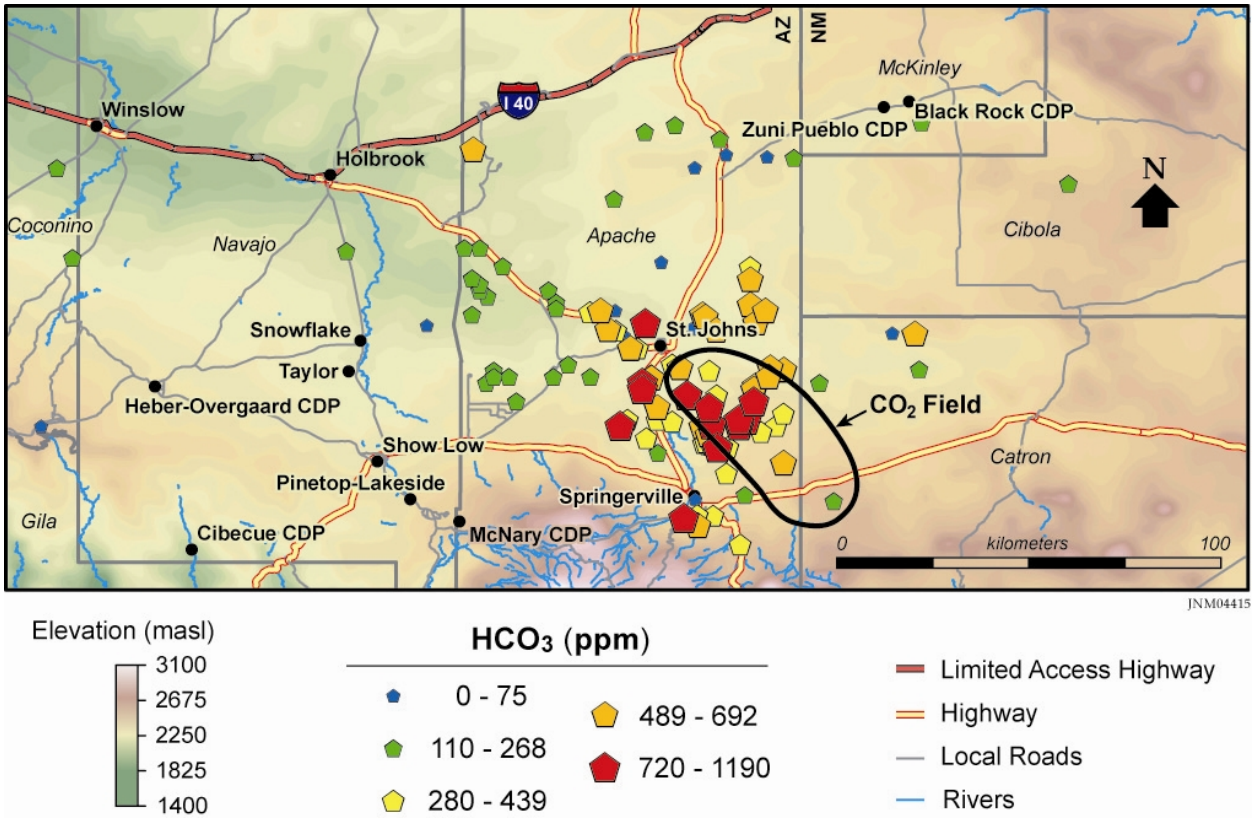

Fig 9. Concentrations of bicarbonate anions from groundwater analyses in the Springerville-St Johns area (from Moore et al., in press).

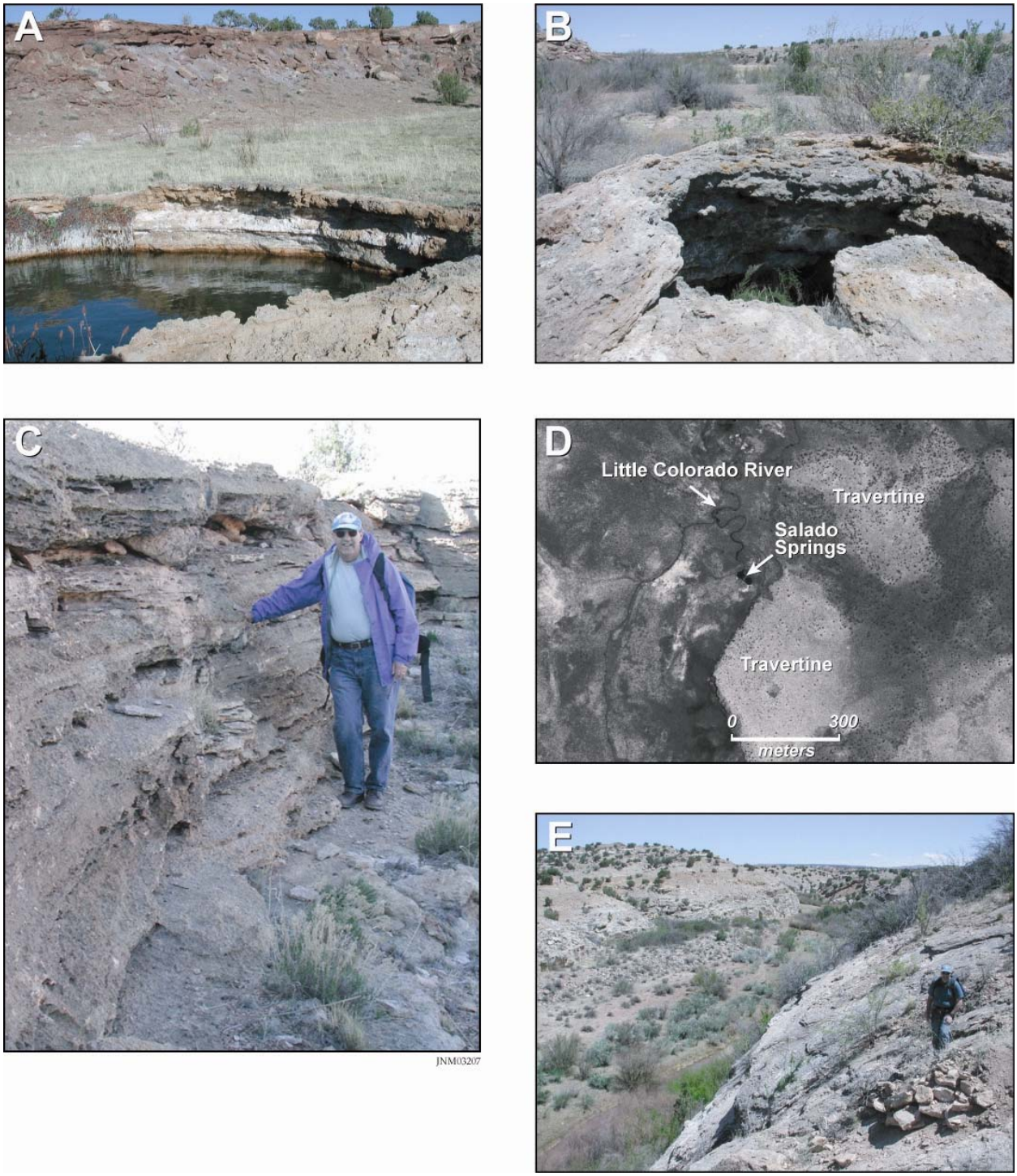

Figure 10. Travertine deposits of the Springerville-St. Johns area. (A) travertine sheets adjacent to Salado Springs. (B) A small well-preserved travertine dome on the valley floor. (C) Interior of a large travertine dome located south of Salado Springs (see D). (D) Areal view of the Salado Springs area showing extensive travertine sheets northeast of the springs and a large dome to the south. The dome's central vent is clearly visible. (E) Travertine sheets on the bluff above Little Colorado River (lower left and center of photo)

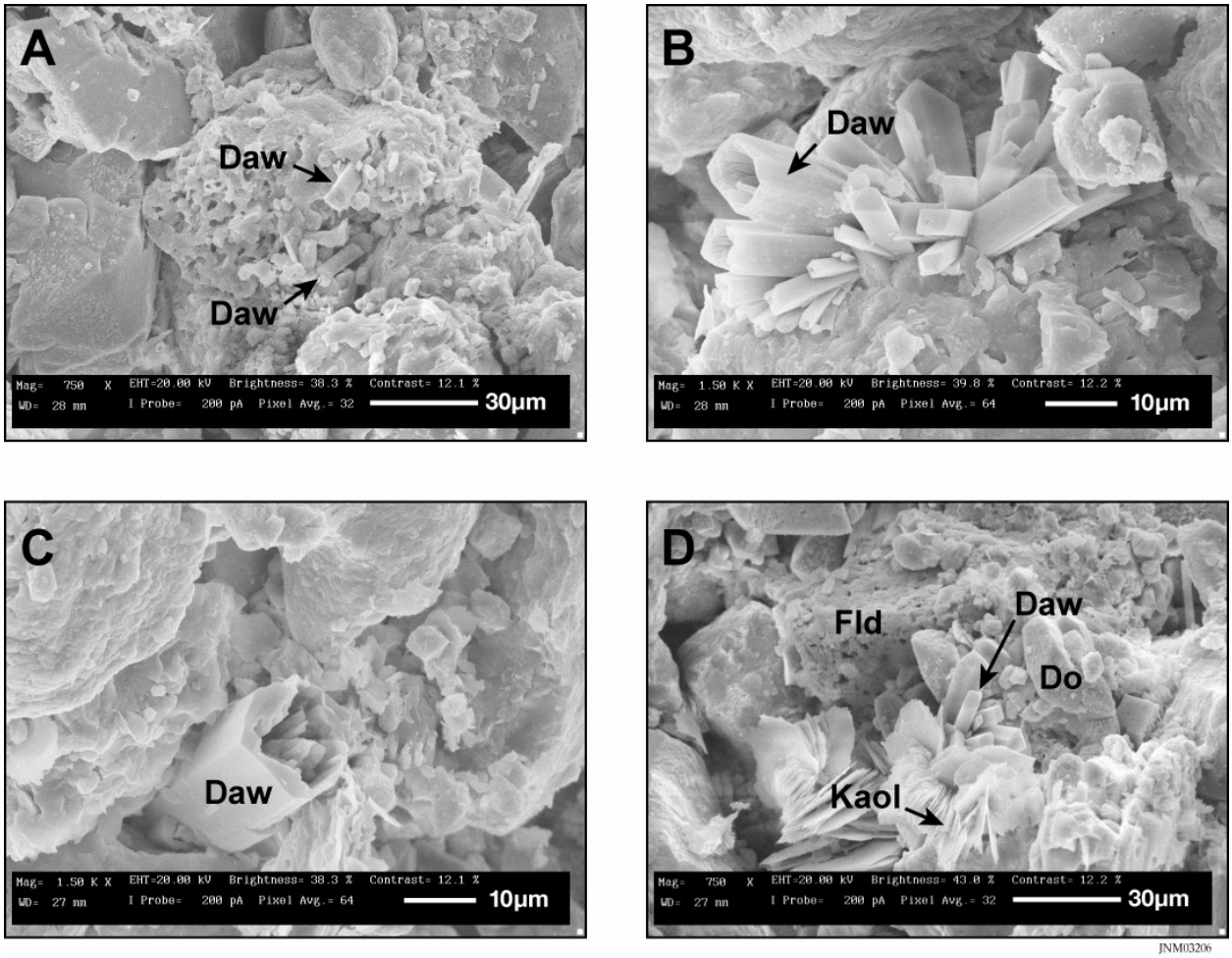

Figure 11. Scanning electron microscope backscattering electron images showing relationships between late-stage authigenic dawsonite and kaolinite from a depth of 468 m in well 22-1X State. (A) Dawsonite growing on weathered potassium feldspar. The feldspar displays dissolution porosity. (B) Dawsonite prisms showing characteristic hollow interiors. The dawsonite crystals have grown on a grain of detrital quartz. (C) Close-up of a hollow dawsonite crystal growing on a surface of a silt grain. There is no corrosion of the crystal's exterior. (D) Pore filling kaolinite and dawsonite. A partially dissolved grain of detrital feldspar projects into the pore space that is lined with early authigenic dolomite. Abbreviations: Daw = dawsonite, do = dolomite, Fld = feldspar, kaol = kaolinite. (From Moore et al., in press).

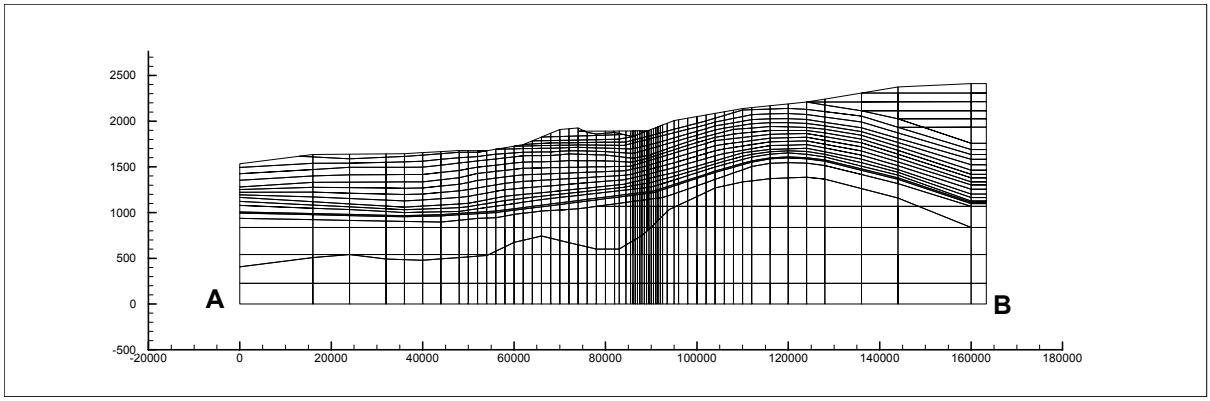

Figure 12: Integrated finite difference grid used in modeling. The wavy lines are the interfaces between geologic units based on the cross section in Fig. 8. Horizontal and vertical axes are in meters. The dense pattern of vertical grid lines in the center of the section allows for a high permeability flow path (fault zone).

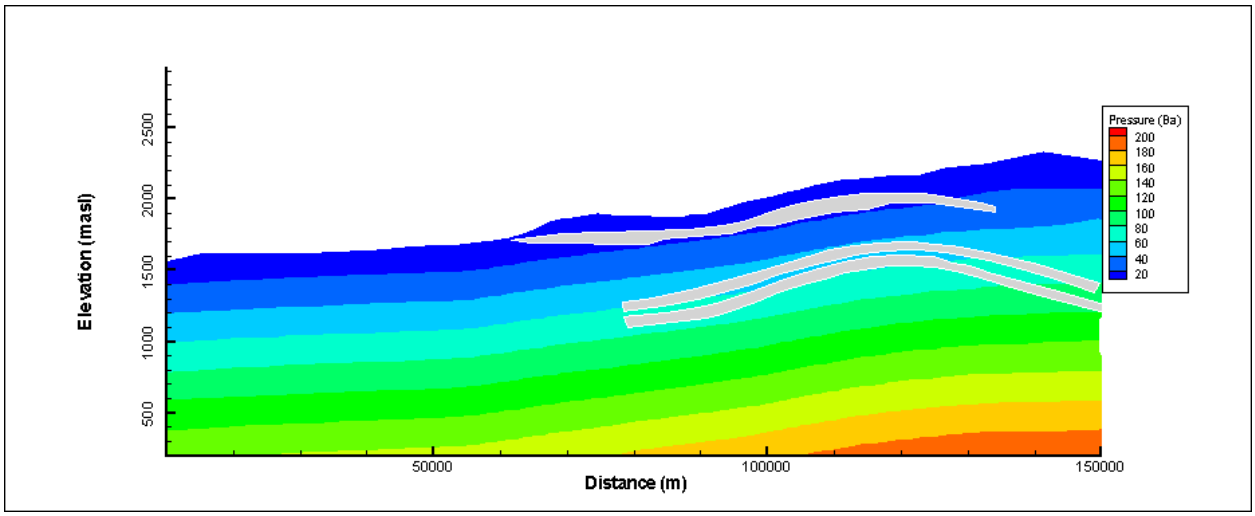

Figure 13: Reservoir pressure and CO_2 deposit location (shown in grey).

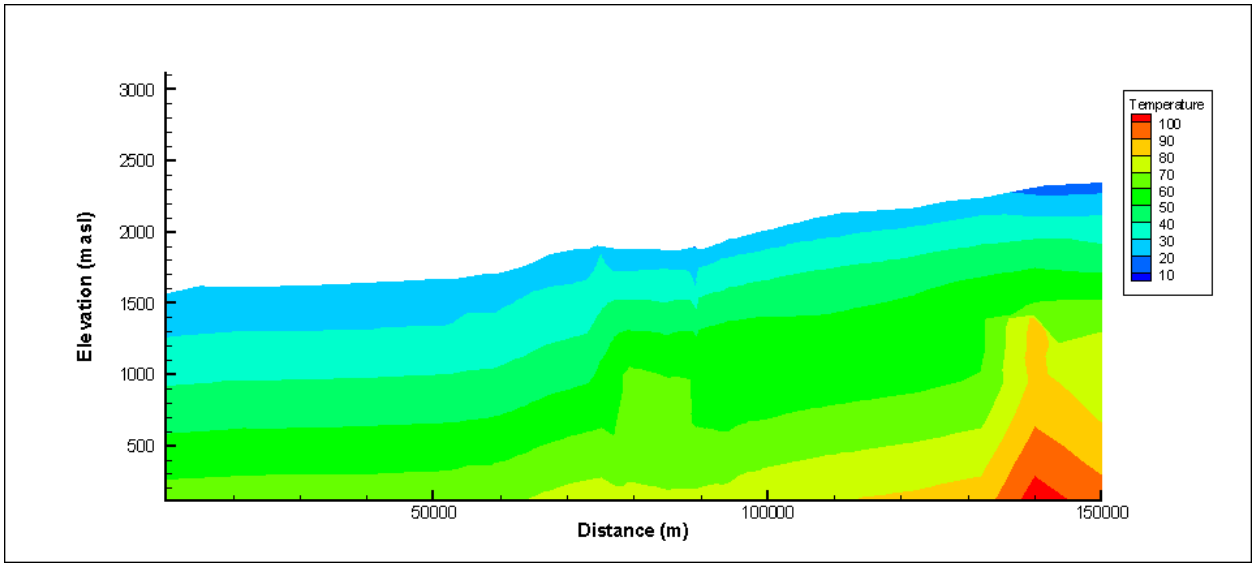

Figure 14: Reservoir temperature.

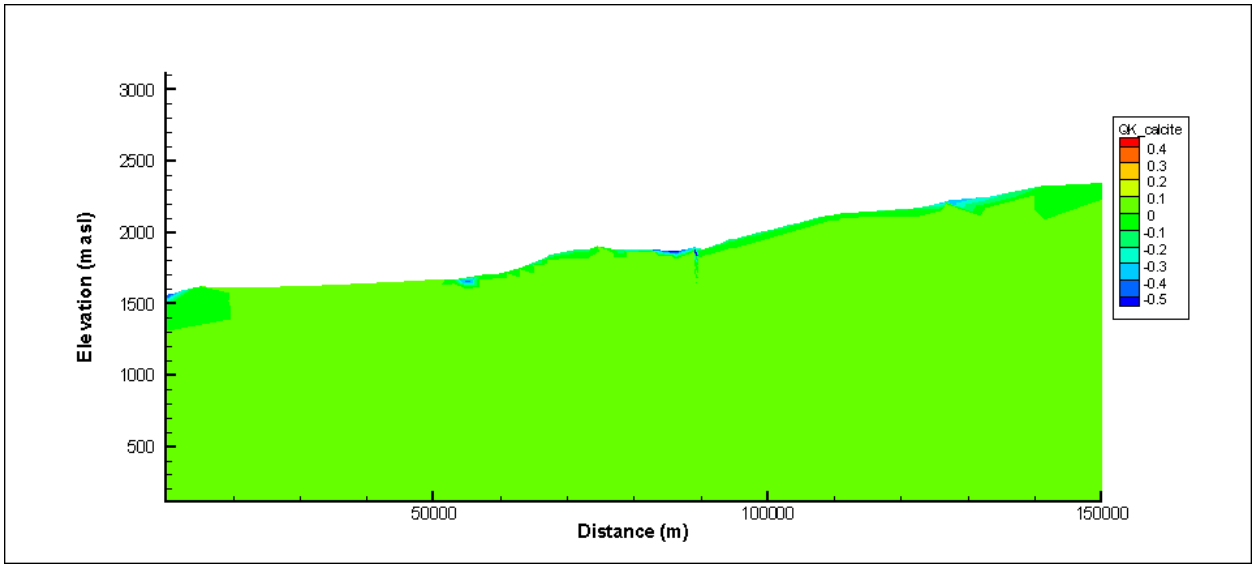

Figure 15: Calcite saturation at 800 years.

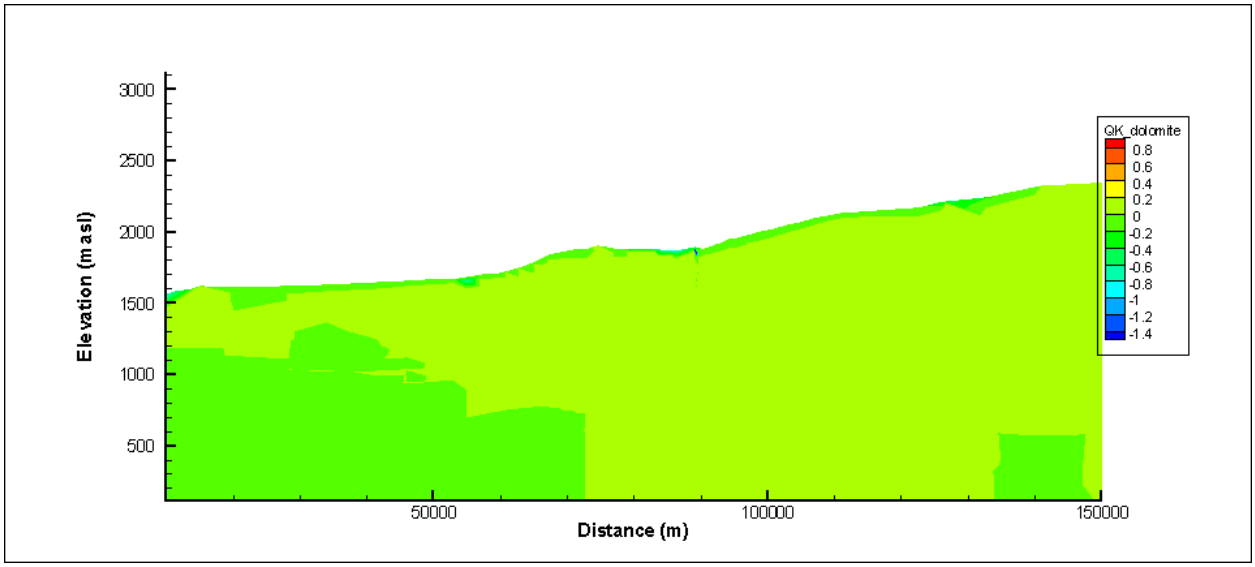

Figure 16: Dolomite saturation at 800 years.

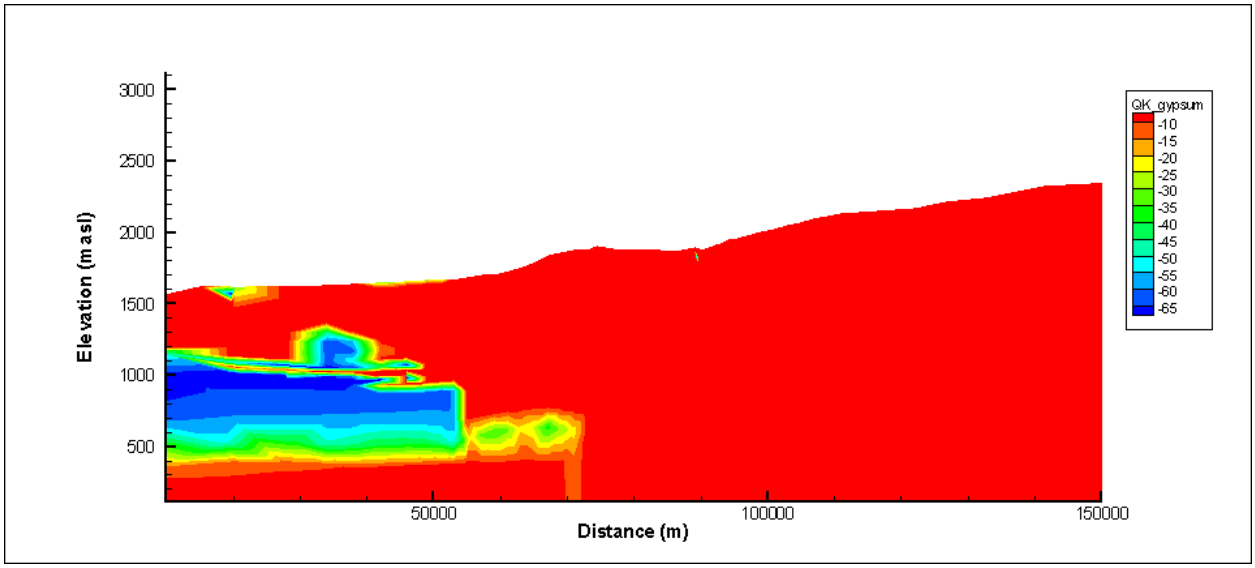

Figure 17: Gypsum saturation at 800 years.

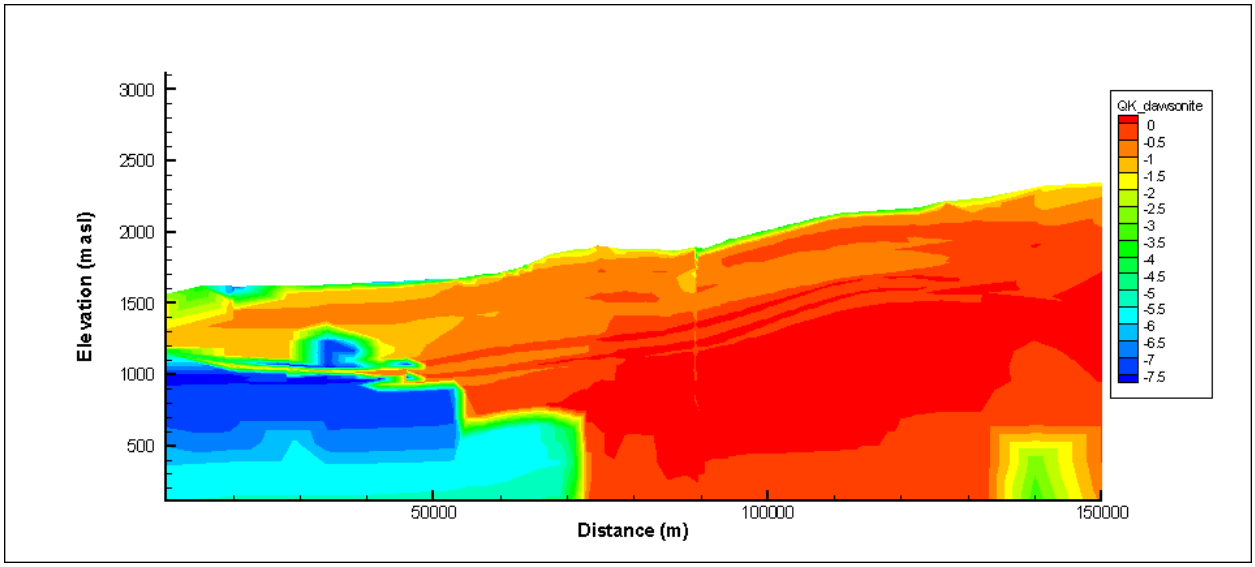

Figure 18: Dawsonite saturation at 800 years.

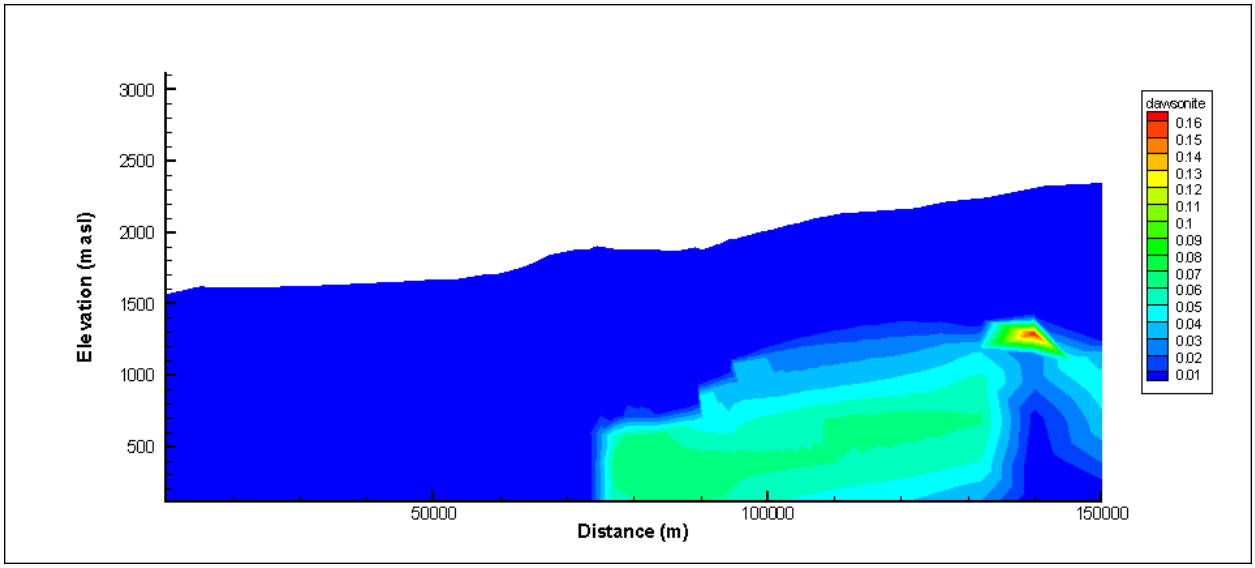

Figure 19: Dawsonite concentration (M/dm^3 of reservoir) at 800 years.

Table 1. Compilation of statistics from the soil gas measurements at Farnham Dome, April, 2004.

Grid #	grid center coords.		grid area (m^2)	site notes
	UTM mW	UTM mN		
1	530950	4377803	33750	mostly shale-derived sediments
2	531542	4377558	8125	mostly shale-derived seds.; partial grid measured
4	535132	4373800	11250	flat area,ss-derived sediments
5	531314	4375959	22500	locally rugged terrain
6	531583	4375905	22500	locally rugged terrain
7	530292	4374487	33750	flat, mostly shale-derived sediments
8	530671	4375695	22500	flat, mostly shale-derived sediments
9	530862	4378481	13125	mixed terrain, visible fault; partial grid measured
10	534923	4367764	22500	mixed terrain
12	531485	4376868	40000	mixed ss hills, shale flats
13	531127	4374944	40000	locally rugged terrain, quartzite, ss, and shales
14	532612	4375428	40000	mixed flat and canyon
15	533611	4374673	40000	flat area, mixed ss and shale-derived sediments
16	533637	4377175	40000	mostly flat with one hill, ss-derived sediments

Grid #	number of measurements	avg. flux	LL_a	UL_{1-a}	std. dev.	max. flux	min. flux	max. temp	min. temp
1	17	0.5	0.2	0.9	0.8	2.4	0.0	16.4	11.6
2	16	0.9	0.6	1.1	0.6	2.4	0.0	19.3	15.7
4	13	1.9	0.6	3.1	2.6	8.6	0.0	11.2	10.1
5	16	3.7	2.9	4.5	1.9	7.4	1.2	16	10.7
6	17	1.4	0.8	2.0	1.4	6.1	0.0	14.2	10
7	21	0.9	0.7	1.2	0.7	1.2	0.0	17.8	11.1
8	21	1.9	1.6	2.3	0.9	2.5	0.2	12.6	8.7
9	18	2.2	1.7	2.6	1.0	3.7	0.0	11.2	8.2
10	40	2.6	2.1	3.0	1.6	2.4	0.0	21.8	13
12	25	2.7	2.1	3.3	1.7	3.6	0.0	20.1	15.2
13	24	3.1	1.9	4.2	3.3	3.6	0.0	22.7	15.1
14	8	2.3	1.4	3.1	1.2	3.7	1.0	12.9	11.1
15	13	1.6	0.6	2.7	2.1	8.6	0.1	11.7	10.3
16	25	1.0	0.7	1.2	0.8	1.2	0.0	19.3	16.3

Note: fluxes are in g m^{-2} d^{-1}; LL and UL are the lower and upper 95% confidence intervals for the means

Table 2: Rock properties used in all simulations.

Formation	**Permeability (m^2)**	**Porosity**
Basement	2.0×10^{-17}	0.02
Amos Wash	6.2×10^{-16}	0.10
Big A Butte	3.5×10^{-15}	0.17
Anhydrite	1.0×10^{-17}	0.05
Fort Apache	8.0×10^{-15}	0.16
Corduory	2.0×10^{-15}	0.16
Glorieta Sandstone	2.0×10^{-13}	0.10
San Andreas Limestone	2.0×10^{-13}	0.10
Moenkopi	2.0×10^{-17}	0.05
Chinle	2.0×10^{-17}	0.05
Volcanics	2.0×10^{-13}	0.10
Basalt	2.0×10^{-15}	0.10
Fault	1.0×10^{-12}	0.30

Table 3. Estimated mineralogy of units from the Springerville-St Johns cross section (vol %)

Formation/Unit	Porosity	Quartz	K-Feldspar	Na Feldspar	Ca Feldspar	Calcite	Dolomite	Gypsum	Na-smectite	Kaolinite	Illite	Hematite	Magnetite	Siderite	Pyrite	TOTAL
Tertiary Volcs.	**20**															
Chinle	**5**	**45**	**1**	**1**	**1**	**2**	**2**		**20**	**20**	**1**	**1**	**1**			**100**
Moenkopi	**5**	**43**	**1**	**1**	**1**	**2**	**5**		**20**	**20**		**2**				**100**
San Andres lst	**10**	**19**				**2**	**65**		**2**	**2**						**100**
Glorieta sst	**20**	**71**	**1**	**1**	**1**	**2**			**2**	**2**						**100**
Supai-Corduroy	**12**	**63**	**4**			**5**	**5**	**15**	**3**	**3**		**2**				**100**
Supai-Fort Apache	**10**	**15**	**1**	**1**		**5**	**45**	**30**	**2**	**1**						**100**
Supai-Big A Butte	**17**	**63**	**2**	**2**		**5**	**5**	**15**	**3**	**3**		**2**				**100**
Supai-Amos Wash	**6**	**63**	**10**	**10**	**2**	**2**			**3**	**3**		**2**	**5**			**100**
Precambrian	**2**	**50**	**10**	**20**	**5**	**4**			**1**	**1**	**1**		**5**		**1**	**100**